Available online at www.sciencedirect.com
ScienceDirect
Polymer 48 (2007) 4352–4360
polymer
www.elsevier.com/locate/polymer

Preparation of multi-walled carbon nanotubes grafted with synthetic poly(L-lysine) through surface-initiated ring-opening polymerization

Jian Li, Wei-Dong He*, Li-Ping Yang, Xiao-Li Sun, Qing Hua

Department of Polymer Science and Engineering, University of Science and Technology of China,
96 Jinzhai Road, Hefei, Anhui 230026, People's Republic of China

Received 5 March 2007; received in revised form 19 May 2007; accepted 29 May 2007
Available online 7 June 2007

Abstract

A surface-initiated ring-opening polymerization approach was used to functionalize multi-walled carbon nanotubes (MWNTs) with linear poly(L-lysine) (PLL). The oxidized MWNTs, which resulted from the treatment of MWNTs with mixed concentrated sulfuric acid and nitric acid, were converted into amino-functionalized MWNTs (MWNT-NH_2) by the amidation of carboxylic group on MWNT surface with excess 1,6-diaminohexane. Surface-initiated ring-opening polymerization of ε-(benzyloxycarbonyl)-L-lysine *N*-carboxyanhydride with MWNT-NH_2 as the initiator resulted in MWNTs grafted with poly(ε-(benzyloxycarbonyl)-L-lysine) (MWNT-*g*-PLys(Z)). After the acidolysis of benzylcarbamate group of the grafting poly(ε-(benzyloxycarbonyl)-L-lysine) chain, water-soluble MWNTs grafted with PLL (MWNT-*g*-PLL) were obtained. The successful grafting was confirmed by Fourier transform infrared spectroscopy, thermal gravimetric analysis, X-ray photoelectron spectroscopy, elemental analyses, high-resolution transmission electron microscopy (HRTEM) and field-emission scanning electron microscopy. HRTEM indicates that MWNTs were enveloped by PLL layer. The as-prepared MWNT-*g*-PLys(Z) and MWNT-*g*-PLL exhibited excellent ability to disperse homogeneously in THF and water, respectively.

Keywords: Multi-walled carbon nanotubes (MWNTs); Surface modification; Poly(L-lysine)

1. Introduction

Carbon nanotubes (CNTs) were first reported by Iijima in 1991 [1]. The great interest concerning with CNTs resides in the possible technological applications as molecular wires, sensors, probes, and biological electronic devices [2–5]. Nevertheless, the processability problem remains a severe hindrance to the extensive applications of CNTs, which explains the recent interests in the functionalization or surface modification of CNTs to improve their processability in a wide range of solvents and the performance of nano-composite materials. The covalent reaction of CNTs with polymers is important because it endows the surfaces with novel structures and properties, and the long polymer chains help the tubes to dissolve in a wide range of solvents.

There are two main methodologies for the covalent attachment of polymeric substances to the surface of CNTs, which are defined as "grafting to" and "grafting from" methods. The former relies on the synthesis of a polymer with a specific end group and the attachment of the polymer chain onto the graphitic surface of the CNTs [6–9]. Its limitation is that the attachment of a small number of chains hinders the diffusion of additional polymer chains to the surface, thereby leading to low grafting density. The "grafting from" method is based on the covalent immobilization of the polymer precursors on the CNT surface and the subsequent polymerization of monomeric species [10–12]. Its advantage is that many kinds of polymer chains with high grafting density are easily attached. Through this methodology, the CNT surface has

---

* Corresponding author. Fax: +86 551 3606743.
E-mail address: wdhe@ustc.edu.cn (W.-D. He).

0032-3861/$ - see front matter © 2007 Elsevier Ltd. All rights reserved.
doi:10.1016/j.polymer.2007.05.076

been modified with polystyrene, poly(acrylic acid), poly(*N*-isopropylacrylamide) and so on [13–17].

Poly(L-lysine) (PLL) is a cationic, biocompatible and biodegradable polymer and its structure facilitates various modifications [18,19] including the conjugation with transferrin, epidermal growth factor, and fusogenic peptides [20,21], thus it has been widely used in the field of gene and drug delivery [22,23]. Synthesis of polypeptide functionalized CNTs has rarely been reported. Zhang et al. [24] prepared PLL-functionalized single-walled carbon nanotubes via a "graft to" method and the application as a biosensor has also been studied.

Recently, a few papers about functionalizing MWNTs via ring-opening polymerization have been reported [13,25,26]. In this work, a surface-initiated ring-opening polymerization approach was used to prepare MWNTs grafted with PLL (MWNT-*g*-PLL) as shown in Fig. 1 and its structure was confirmed by FTIR, TGA, XPS, HRTEM and FESEM measurements. Such a molecular nanohybrid (MWNT-*g*-PLL) has many advantages such as good solubility in water and a tube surface with amino groups. MWNT-*g*-PLL could have potential applications in delivery systems and biosensors. Other polypeptide functionalized MWNTs can also be prepared through this strategy.

2. Experimental section

2.1. Materials

The MWNTs used were purchased from Sun Nanotech Co. Ltd. in Nanchang, Jiangxi, and the purity is higher than 90%. THF was dried over sodium/benzophenone and distilled just before use. *n*-Hexane was dried and distilled over CaH_2 before use. Triethylamine was stirred with KOH for 12 h at room temperature, refluxed with toluene-4-sulfonyl-chloride and distilled before use. 1,6-Diaminohexane and 4-(dimethylamino)pyridine were ACROS reagents. Triphosgene, trifluoroacetic acid, methanesulfonic acid, anisole and ε-(benzyloxycarbonyl)-L-lysine were all Sigma–Aldrich reagents. Those chemicals were used without further purification. The PLL homopolymer used was prepared according to a reported procedure [27].

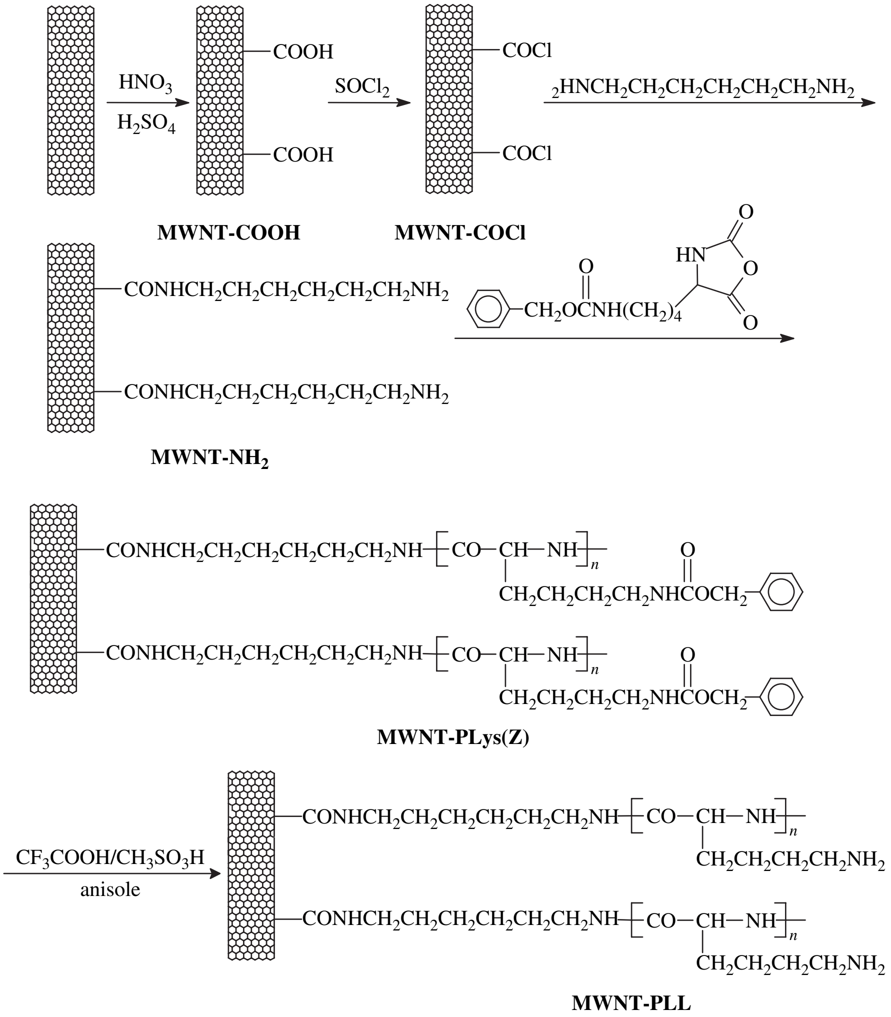

Fig. 1. Outline of PLL chain attached to MWNTs.

2.2. Experimental procedures

2.2.1. Synthesis of MWNT-COOH

MWNTs (0.30 g) were suspended in 20 ml of a 3:1 (v) mixture of concentrated H_2SO_4 (98 wt%)/HNO_3 (60 wt%). The above mixture was sonicated in a water bath for 2 h, and stirred for 15 h at 35 °C. Then the mixture was diluted with 100 ml of distilled water, vacuum-filtered and washed with distilled water until pH of the filtrate was 7.0. The filtered solid was dried under vacuum for 20 h at 60 °C, obtaining carboxyl-functionalized MWNTs (MWNT-COOH) (0.28 g).

2.2.2. Synthesis of MWNT-NH_2

Amine functionalized MWNTs (MWNT-NH_2) were prepared as follows. A 250 ml round-bottomed flask was charged with 0.3 g of MWNT-COOH and 30 ml of $SOCl_2$. The mixture was stirred at 80 °C for 24 h and the unreacted $SOCl_2$ was removed under vacuum. The remaining solid (MWNT-COCl) was washed three times with anhydrous THF and vacuum-dried at 35 °C for 4 h. The as-produced MWNT-COCl was added to 10 g of 1,6-diaminohexane at 35 °C, sonicated in a water bath for 30 min, then reacted at 65–75 °C for 24 h in the presence of triethylamine and 4-(dimethylamino)-pyridine. MWNT-NH_2 (0.25 g) was obtained after repeated washing with hexane, filtration, and vacuum-drying [28,29].

2.2.3. Synthesis of MWNT-*g*-PLys(Z)

ε-Benzyloxycarbonyl-L-lysine *N*-carboxyanhydride (Lys(Z)-NCA) was synthesized by the Fuchs–Farthing method using triphosgene [30,31].

MWNT-*g*-PLys(Z) was prepared as follows. MWNT-NH_2 (60 mg) was suspended in 20 ml of anhydrous THF and the mixture was sonicated in a water bath for 30 min. Lys(Z)-NCA (1.0 g) was dissolved in 20 ml of anhydrous THF and then added into MWNT-NH_2 suspension. The reaction stood at 30 °C for 48 h under inert atmosphere. Then the mixture was diluted with 80 ml of THF, sonicated for 10 min, and filtered through a 0.2-μm PTFE membrane. The solid was further washed with THF to remove the free polymer. After five washings, no cloudiness was observed when five drops of the filtrate were added into 10 ml of diethyl ether, indicating that almost no homopolymer of PLys(Z) remained in the so-purified product. The product was vacuum-dried for 24 h to give MWNTs grafted with PLys(Z) (MWNT-*g*-PLys(Z)2 in Table 1).

2.2.4. Acidolysis of benzylcarbamate group from MWNT-*g*-PLys(Z)

MWNT-*g*-PLys(Z)2 (60 mg) was added to 5 ml of trifluroacetic acid and stirred for 0.5 h. The suspension was added to 5 ml of anisole and 3.5 ml of methanesulfonic acid, and the mixture was stirred for 1.5 h. Subsequently, the suspension was diluted with 60 ml of distilled water and vacuum-filtered. After neutralizing with triethylamine aqueous solution, three washings with distilled water and vacuum-drying for 24 h, the black solid of MWNTs grafted with poly(L-lysine) (MWNT-*g*-PLL2 in Table 1) was obtained.

Table 1
Preparation of PLys(Z)-grafted MWNTs and PLL-grafted MWNTs

Sample	R_{feed}[a] Lys(Z)-NCA:MWNT	Polymer[c] (wt%)	Thickness of polymer layer[d] (nm)
MWNT-*g*-PLys(Z)2	16.67:1	54	15.5
MWNT-*g*-PLL2[b]	16.67:1	36.9	11.0
MWNT-*g*-PLys(Z)1	8.33:1	27.2	6.0

[a] The feed ratio of Lys(Z)-NCA (g) to MWNT-NH_2 (g).

[b] The MWNT-*g*-PLL2 was obtained by the benzylcarbamate acidolysis of MWNT-*g*-PLys(Z)2.

[c] The polymer content calculated from TGA weight loss.

[d] The average thickness of the polymer shell was measured by HRTEM. The data from 10 carbon nanotubes were averaged.

2.3. Characterization

Fourier transform infrared (FTIR) spectra were recorded on a Bruker VECTOR-22 IR spectrometer in KBr pellets. Thermal gravimetric analyses (TGA) were carried out on a PE TGA-7 instrument with a heating rate of 20 °C/min in a nitrogen atmosphere. Elemental analyses were performed on a Vario EL-III Elementar. X-ray photoelectron spectroscopy (XPS) was recorded on an ESCALAB MKII photoelectron spectrometer using non-monochromatic Al Kα radiation (1486.6 eV) under ultra-high-vacuum (about 10^{-11} mbar). Field-emission scanning electron microscope (FESEM) analysis was conducted on a JSM-6700F electron microscope at 5 kV and the samples were loaded on a glass surface previously sputter-coated with a homogeneous gold layer for charge dissipation during the SEM imaging. Transmission electron microscopy (TEM) and high-resolution transmission electron microscopy (HRTEM) observations were conducted on a Hitachi model H-800 and a JEOL 2010 electron microscope, respectively. The samples for TEM and HRTEM without staining were prepared by placing one drop of MWNT dispersion in THF onto carbon-coated copper grids. For HRTEM observation with staining, one drop of MWNT dispersion in THF (MWNT-*g*-PLys(Z)1 and MWNT-*g*-PLys(Z)2) or water (MWNT-*g*-PLL2) was placed on carbon-coated copper grids. After the solvent evaporated naturally, the above carbon-coated copper grids were dropped with one drop of 1 wt% aqueous solution of phosphotungstic acid and dried under ambient condition.

3. Results and discussion

3.1. Initiator immobilization on MWNT surface

Amine groups are the initiators for the ring-opening polymerization of Lys(Z)-NCA, so we immobilized 1,6-diaminohexane onto MWNTs to graft MWNT with PLL. MWNTs were first oxidized with nitric acid (60%) and sulfuric acid (98%). The oxidized MWNTs (MWNT-COOH) were converted into acyl chloride-functionalized MWNTs (MWNT-COCl) in neat thionyl chloride. MWNT-COCl was reacted with excess 1,6-diaminohexane, affording amino-functionalized MWNTs (MWNT-NH_2).

The FTIR spectrum (Fig. 2A) of MWNT-NH_2 clearly shows the characteristic stretching vibrations of C–H and C=O

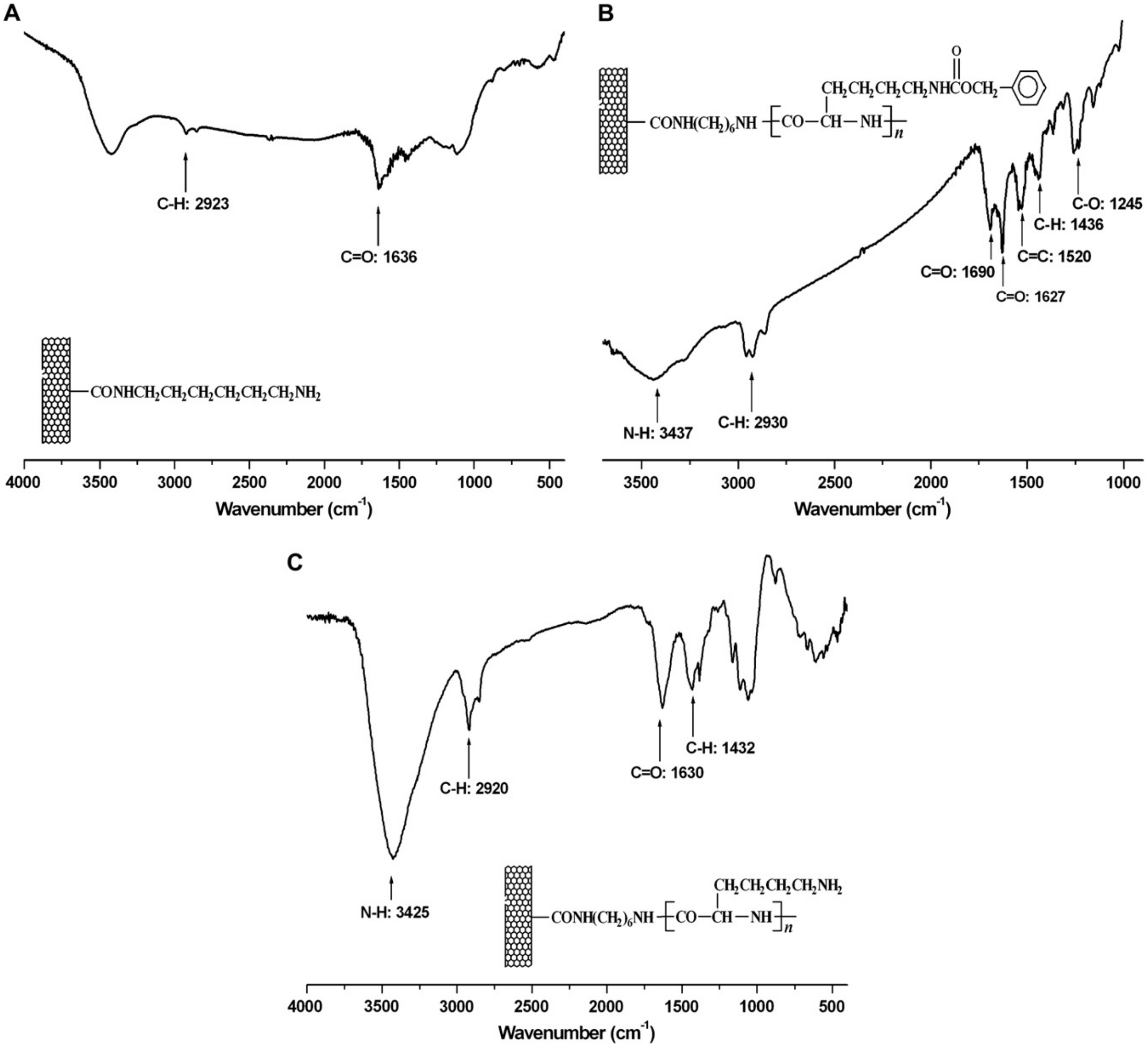

Fig. 2. FTIR spectrum of different MWNTs (MWNT-NH_2 (A); MWNT-*g*-PLys(Z)2 (B); MWNT-*g*-PLL2 (C)).

centered at 2923 cm^{-1} and 1636 cm^{-1}, respectively. The XPS spectrum of MWNT-NH_2 is shown in Fig. 3a. The major signal at the binding energy (BE) of about 284.60 eV is assigned to C_{1s}, the minor signal at the BE of 533.30 eV is attributed to O_{1s} on the surface of the MWNTs, and the small peak at the BE of 400.25 eV corresponds to N_{1s} of the 1,6-diaminohexane attached to MWNTs. The XPS results revealed about 0.81 mmol of amino groups per gram of MWNT-NH_2 calculated from the intensity of the N_{1s} peaks. TGA results (Fig. 4b) showed a weight loss of MWNT-NH_2 due to the attached 1,6-diaminohexane in the temperature range of 270–440 °C and about 0.75 mmol of amino groups per gram of MWNTs based on the weight loss (9.3%), which was similar to the value obtained from XPS.

The element analysis of MWNT-NH_2 follows.

Calculated value based on TGA: C, 88.70; N, 2.05; H, 1.26.
Found by element analysis: C, 88.43; N, 1.98; H, 1.26.

For these reasons, we conclude that 1,6-diaminohexane was covalently bound onto the surface of MWNTs. Since an extreme excess of 1,6-diaminohexane was used in this reaction, free primary amine groups should remain on the MWNT surface.

3.2. Growth of PLys(Z) chains from MWNTs via surface-initiated ring-opening polymerization and conversion of MWNT-g-PLys(Z) into MWNT-g-PLL

In this study, the primary amine group on the surface of MWNT-NH_2 was used as the initiator for ring-opening polymerization of Lys(Z)-NCA in THF. To ensure that most of the amines initiate the polymerization, MWNT-NH_2 in THF should be sonicated for an adequate period of time. After the polymerization, the homopolymers not bound to MWNTs were removed by washing thoroughly with THF until no

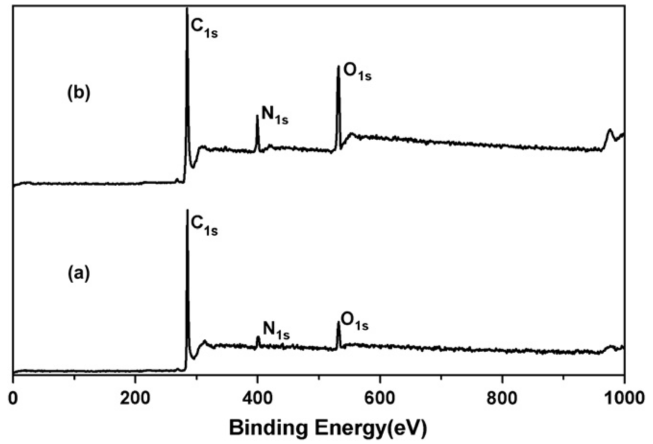

Fig. 3. XPS spectrum of MWNT-NH_2 (a) and MWNT-PLL2 (b).

polymer was found in the filtrate. The weight of MWNT-*g*-PLys(Z) obtained was greater than that of MWNT-NH_2 used, suggesting the surface attachment of PLys(Z) via ring-opening polymerization. Trifluoroacetic acid/methanesulfonic acid/anisole were used to remove the benzylcarbamate groups from MWNT-*g*-PLys(Z). After the de-protection, the reaction mixture was diluted with water and the resultant products were filtered and washed with water to remove the acids and organic solvent. MWNT-*g*-PLL was collected as black powder.

3.3. Characterization of MWNT-g-PLys(Z) and MWNT-g-PLL

To determine the polymer content in the CNT composites, TGA measurements were performed on the functionalized MWNTs. Fig. 4a shows that the pristine MWNTs started to decompose at 620 °C under nitrogen atmosphere. Besides the weight loss due to the attached hexanediamine of MWNT-NH_2, the major endothermic process appeared in the temperature range 600–680 °C, assigned to the thermal decomposition of oxidized MWNTs. TGA analysis of MWNT-*g*-PLys(Z)2 shows that the thermal decomposition corresponding to the surface-attached PLys(Z) on MWNTs occurred in the temperature range 200–500 °C, and that due to oxidized MWNTs in the temperature range 520–710 °C. The weight percents of PLys(Z) attached to MWNT determined by TGA (Fig. 4c and f) were 29% and 54% for MWNT-*g*-PLys(Z)1 and MWNT-*g*-PLys(Z)2, respectively, indicating that the amount of PLys(Z) attached to MWNTs can be altered by adjusting the feed ratio of monomer to MWNT-NH_2. From the TGA curves of MWNT-*g*-PLys(Z)1 and MWNT-*g*-PLys(Z)2, we can also see that the decomposition temperature of the grafted PLys(Z) increases with increasing graft content. The TGA of MWNT-*g*-PLL2 is shown as Fig. 4d and the weight percent of PLL was 36.9% based on the weight loss from the decomposition of PLL, which was in accordance with the calculated value of 36.6% based on the composition of MWNT-*g*-PLys(Z)2.

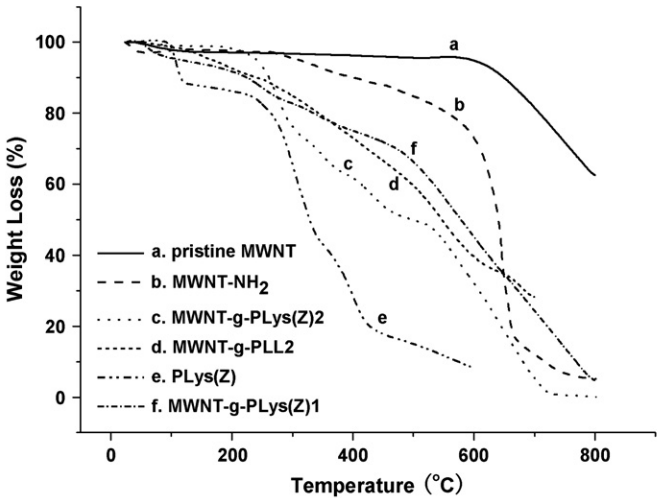

Fig. 4. TGA curves of different MWNTs (pristine MWNT (a); MWNT-NH_2 (b); MWNT-*g*-PLys(Z)2 (c); MWNT-*g*-PLL2 (d); PLys(Z) (e); MWNT-*g*-PLys(Z)1 (f)).

The XPS spectrum of MWNT-PLL2 is shown in Fig. 3b. The intensities of the major signals of N_{1s} and O_{1s} were greatly increased compared with Fig. 3a, which indicated the grafting of PLL onto MWNTs.

The chemical structures of the resulting nano-composites of MWNT-*g*-PLys(Z) and MWNT-*g*-PLL were further confirmed by FTIR measurement, which can provide rich information about the functional groups grafted onto the sidewall of MWNTs. The FTIR spectrum of MWNT-*g*-PLys(Z)2 (Fig. 2B) exhibits the characteristic vibration bands for PLys(Z): N–H at 3437 cm^{-1}; C–H at 2930 cm^{-1} and 1436 cm^{-1}; C=O at 1690 cm^{-1} and C–O at 1245 cm^{-1} were attributed to the benzylcarbamate groups; C=O at 1627 cm^{-1} was attributed to the amide group closest to MWNTs; C=C at 1520 cm^{-1} was attributed to phenyl groups. The FTIR spectrum of MWNT-*g*-PLL2 (Fig. 2C) exhibits the characteristic vibration bands of PLL such as N–H at 3425 cm^{-1}; C=O at 1630 cm^{-1}; C–H at 2920 cm^{-1} and 1432 cm^{-1}. The disappearance of benzylcarbamate bands at 1690 cm^{-1} and 1520 cm^{-1} showed that the benzylcarbamate groups in MWNT-*g*-PLys(Z)2 were removed from the surface of MWNT.

Fig. 5 shows the solubility of pristine MWNTs, MWNT-NH_2, MWNT-*g*-PLys(Z)1 and MWNT-*g*-PLys(Z)2 in THF, and MWNT-*g*-PLL2 in water. It is clear that pristine MWNTs and MWNT-NH_2 are insoluble in THF, and there is much sediment at the vial bottom. Homogeneous dispersion of MWNT-NH_2 in an organic solvent or aqueous solution was very difficult even after the carbon nanotubes had been subjected to sonication. Sedimentation of MWNT-NH_2 from THF appeared a few minutes after sonication. On the contrary, MWNT-*g*-PLys(Z)1 and MWNT-*g*-PLys(Z)2 are soluble in THF, and MWNT-*g*-PLL2 in water, forming a homogeneous dispersion; there was no sedimentation observed even after ten days as shown in Fig. 5D–F. As a comparison, we attempted to disperse the mixture of MWNT-NH_2 (65 wt%) and PLL (35 wt%) in water, and the mixture was subjected to sonication for about 30 min. After the storage for 20 min, MWNTs precipitated out (Fig. 5C), suggesting that the good solubility of

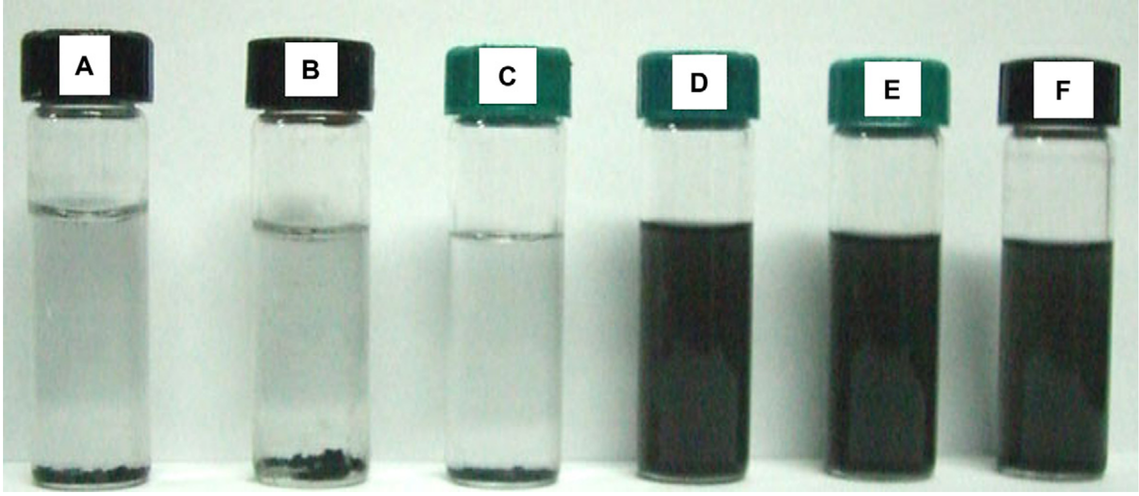

Fig. 5. Photographs of MWNT samples: pristine MWNTs in THF (A); MWNT-NH_2 in THF (B), the concentration of samples A and B is 0.3 g/l; mixture of MWNT-NH_2 (65 wt%) and PLL (35 wt%) in water (C), the total concentration is 1 g/l; MWNT-*g*-PLys(Z)2 in THF (D); MWNT-*g*-PLL2 in H_2O (E); MWNT-*g*-PLys(Z)1 in THF (F). All photos were taken after 10 days of storage at room temperature. The concentration of functionalized MWNTs of samples D–F is 0.3 g/l.

polymer-functionalized MWNTs is due to the covalent bonding of PLL and PLys(Z) chains instead of their physisorption onto the surface of MWNTs.

3.4. Morphology of the polymer-grafted MWNTs

TEM, especially high-resolution TEM (HRTEM), is a powerful tool for characterizing nanomaterials such as CNTs and polymer-functionalized CNTs [32–35]. Using HRTEM, core–shell structure of polymer-grafted MWNTs is not difficult to observe, and the thickness of the polymer shell can be measured. The TEM images of pristine MWNTs are shown in Fig. 6. The average internal and external diameters of the MWNTs are 5–10 nm and 20–35 nm, respectively. The length of the MWNTs is approximately several micrometers. MWNTs were piled up to form large bundles and ropes.

Fig. 7A shows the HRTEM images of MWNT-*g*-PLys(Z)2 without staining. The expected core–shell structure of PLys(Z)-grafted MWNTs was obscurely identified, probably due to the poor contrast between the PLys(Z) shell and the background. Therefore, the phosphotungstic acid staining technique was used to improve the contrast. Fig. 7B–E shows the typical HRTEM images of polymer-functionalized MWNTs. The core–shell structure of the MWNT-*g*-PLys(Z)2 (Fig. 7B), MWNT-*g*-PLL2 (Fig. 7C and D) and MWNT-*g*-PLys(Z)1 (Fig. 7E) with MWNTs at the center can be clearly observed, indicating that the MWNTs were coated by a layer of polymer chains [36,37]. The thicknesses of the

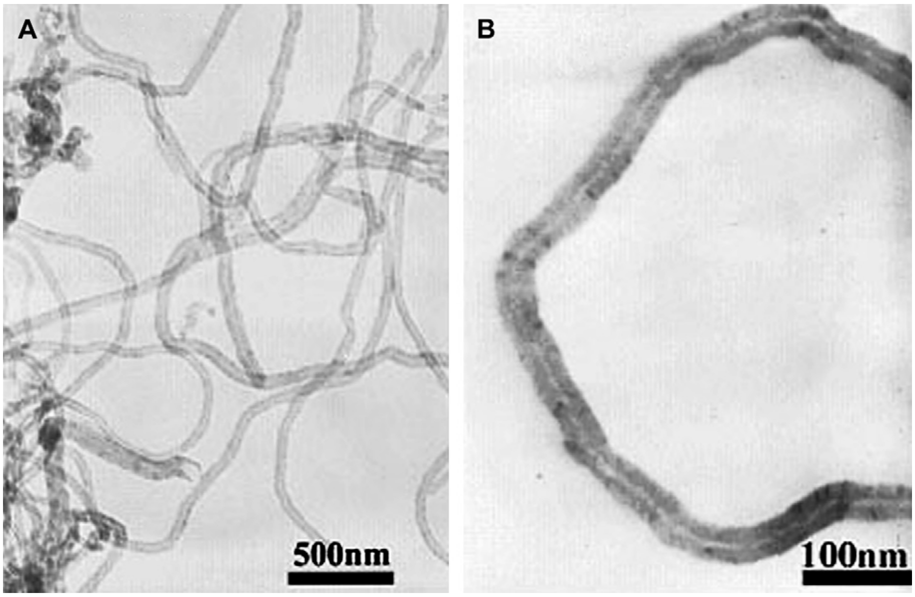

Fig. 6. TEM images of pristine MWNTs.

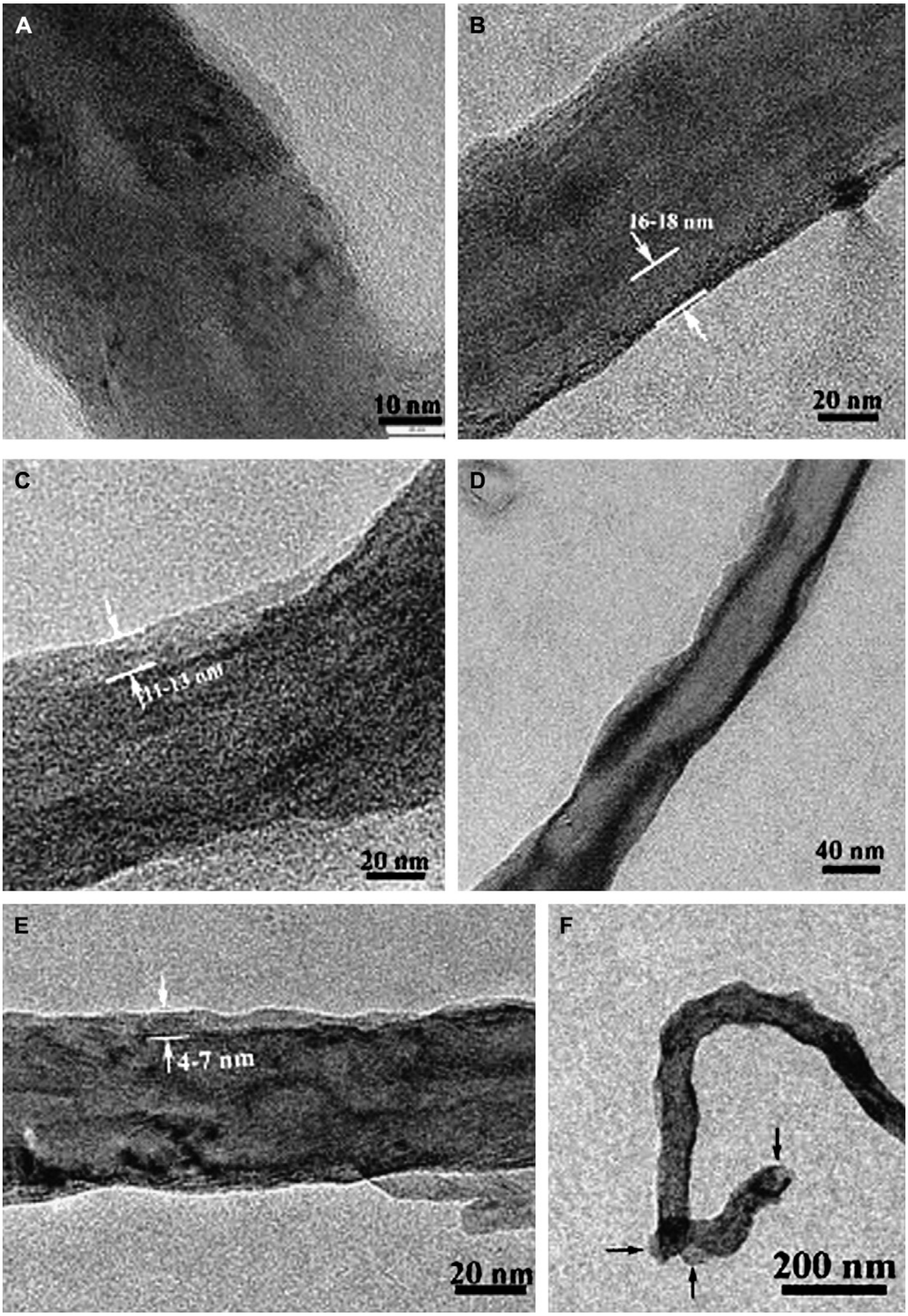

Fig. 7. HRTEM images of MWNT-*g*-PLys(Z)2 without staining by phosphotungstic acid (A); HRTEM images of MWNT-*g*-PLys(Z)2 (B and F), MWNT-*g*-PLL2 (C and D) and MWNT-*g*-PLys(Z)1 (E), stained by phosphotungstic acid.

polymer shell shown in Fig. 7B, C and E (marked by the white arrows) are 16–18 nm, 4–7 nm, and 11–13 nm, respectively. The average thickness of the grafted polymer layer measured by HRTEM is listed in Table 1 and 10 carbon nanotubes were counted. It is found that greater the amount of grafted polymer produce, thicker the polymer shells. As reported previously [38,39], the ends and bends of CNTs, having stronger reactivity, exhibited more defects and heptagons [40]. Thus, the polymer layer at the bends and ends was rather thicker than that on the straight sections of the tube. This

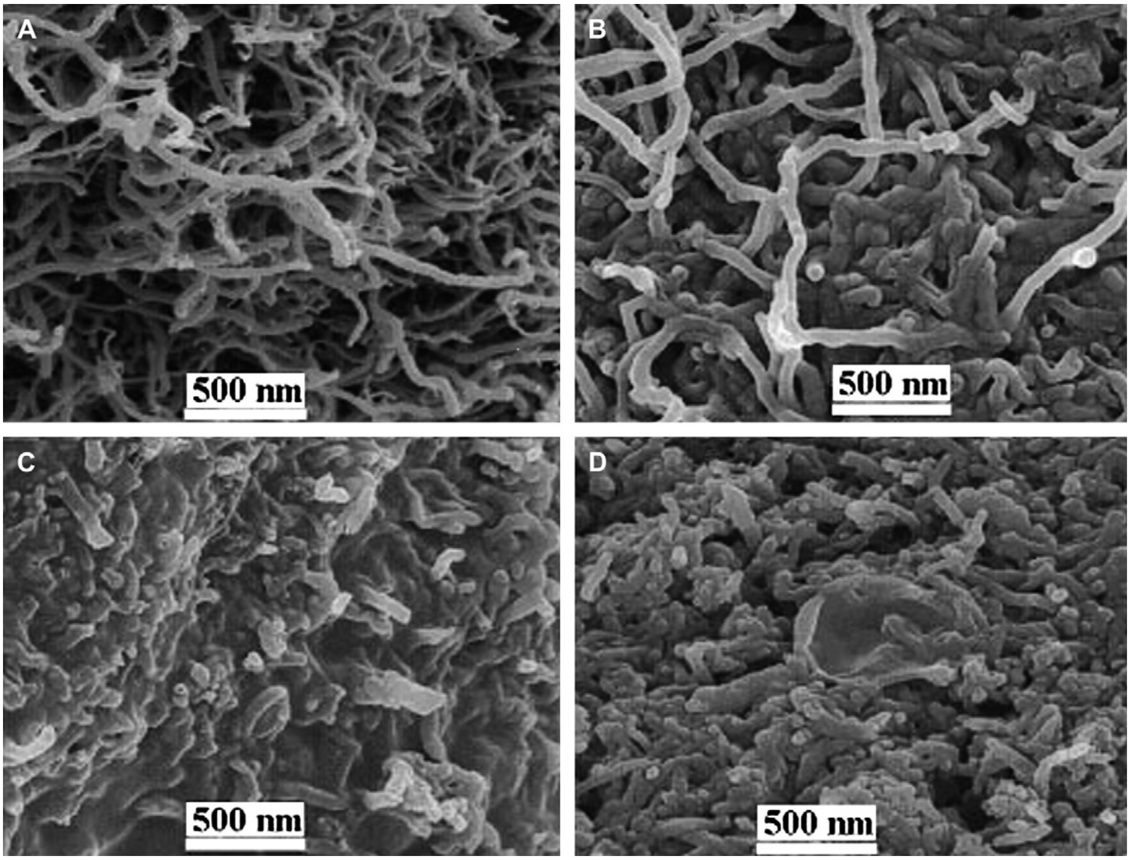

Fig. 8. Field-emission SEM images of the pristine MWNTs (A); MWNT-*g*-PLys(Z)1 (B); MWNT-*g*-PLys(Z)2 (C); MWNT-*g*-PLL2 (D). Samples were obtained by directly drying the THF solution of MWNT-*g*-PLys(Z) or water solution of MWNT-*g*-PLL2.

phenomenon was clearly observed in Fig. 7F (marked by the black arrows).

The bulk nanostructures and morphology of the samples were observed with field-emission scanning electron microscopy (FESEM), as shown in Fig. 8. Generally, the PLys(Z) and PLL-functionalized tubes look thicker compared to the pristine nanotubes. For the sample MWNT-PLys(Z)1 (Fig. 8B), rod-like nanostructures can still be clearly observed [25,41]. As the amount of grafted polymer increases, the distances among the tubes become narrower, and the polymer phase becomes more continuous, the rods become less distinct with eventually only a compact mass being observed (see Fig. 8C). For the sample MWNT-PLL2 (Fig. 8D), the polymer phase becomes less continuous and the wrapping of tubes by polymers is less than that of MWNT-PLys(Z)2, due to the acidolysis of benzylcarbamate group from MWNT-*g*-PLys(Z)2. All of the aforementioned characterizations are in accordance with the FESEM results, confirming the successful grafting of PLL onto MWNT surface.

4. Conclusions

MWNTs were covalently functionalized with poly(L-lysine) by the surface-initiated ring-opening polymerization strategy. The grafted polymer content can be controlled by adjusting the feed ratio of the Lys(Z)-NCA monomer to MWNTs. Characterization of the MWNT nano-composites by FTIR, TGA and XPS revealed the covalent linkage between the polymers and the MWNT surface. A core–shell nanostructure was observed under HRTEM with phosphotungstic acid staining and the MWNTs were enveloped by the polymer layers. The thickness of the polymer layer increased with increasing the grafted polymer quantity. The bulk nanostructure of the composites was observed using FESEM, which confirmed the successful grafting of PLL onto MWNT surface. The as-prepared MWNT-*g*-PLys(Z) and MWNT-*g*-PLL exhibit excellent dispersibility in THF and water, respectively. The method reported in this paper can be extended to graft MWNTs with various polypeptides such as poly(L-aspartic acid) and poly(L-threonine) to offer MWNTs different biological features and various groups for further functionalization on the surface of MWNTs.

Acknowledgements

Financial supports by State Key Laboratory of Polymer Physics and Chemistry and Anhui Nature Science Foundation are greatly acknowledged.

References

[1] Iijima S. Nature (London) 1991;354(6348):56–8.

[2] Baughman RH, Zakhidov AA, de Heer WA. Science 2002;297(5582):787–92.

[3] Kleckley S, Chai GY, Zhou D, Vanfleet R, Chow L. Carbon 2003;41(4):833–6.

[4] Yoon SH, Jin HJ, Kook MC, Pyun YR. Biomacromolecules 2006;7(4):1280–4.

[5] Lefebvre J, Antonov RD, Radosavljevi M, Lynch JF, Llaguno M, Johnson AT. Carbon 2000;38(11–12):1745–9.

[6] Mansky P, Liu Y, Huang E, Russell TP, Hawker CJ. Science 1997;275(5305):1458–60.

[7] Blake R, Gun'ko YK, Coleman J, Cadek M, Fonseca A, Nagy JB, et al. J Am Chem Soc 2004;126(33):10226–7.

[8] Qin S, Qin D, Ford WT, Resasco DE, Herrera JE. Macromolecules 2004;37(3):752–7.

[9] Liu IC, Huang HM, Chang CY, Tsai HC, Hsu CH. Macromolecules 2004;37(2):283–7.

[10] Hong CY, You YZ, Pan CY. Polymer 2006;47(12):4300–9.

[11] Qin S, Qin D, Ford WT, Zhang Y, Kotov NA. Chem Mater 2005;17(8):2131–5.

[12] Baibarac M, Baltog I, Godon C, Lefrant S, Chauvet O. Covalent functionalization of single-walled carbon nanotubes by aniline electrochemical polymerization. Carbon 2004;42(15):3143–52.

[13] Xu YY, Gao C, Kong H, Yan D, Jin YZ. Macromolecules 2004;37(24):8846–53.

[14] Liu YQ. Macromolecules 2004;37(13):4755–60.

[15] Park SJ, Cho MS, Lim MS, Choi HJ, Jhon MS. Macromol Rapid Commun 2003;24(18):1070–3.

[16] Viswanathan G, Charapani N, Yang H, Wei B, Chung H, Cho K, et al. J Am Chem Soc 2003;125(31):9258–9.

[17] Baskaran D, Mays JW, Bratcher MS. Angew Chem Int Ed 2004;43(16):2138–42.

[18] Winblade ND, Nikolic ID, Hoffman AS, Hubbell JA. Biomacromolecules 2000;1(4):523–33.

[19] Park S, Healy KE. Bioconjugate Chem 2003;14(2):311–9.

[20] Vishalakshi B, Ghosh S, Kalpagam V. Polymer 1993;34(15):3270–5.

[21] Taxman DJ, Lee ES, Wojchowski DM. Anal Biochem 1993;213(1):97–103.

[22] Ferdous A, Akaike T, Maruyama A. Biomacromolecules 2000;1(2):186–93.

[23] Subr V, Konak C, Laga R, Ulbrich K. Biomacromolecules 2006;7(1):122–30.

[24] Zhang YJ, Li J, Shen YF, Wang MJ, Li JH. J Phys Chem B 2004;108(39):15343–6.

[25] Zeng HL, Gao C, Yan DY. Adv Funct Mater 2006;16(6):812–8.

[26] Chen GX, Kim HS, Park BH. Macromol Chem Phys 2007;208(4):389–98.

[27] Harada A, Kataoka K. J Macromol Sci Pure Appl Chem 1997;A34(10):2119–33.

[28] Gao C, Walton DRM. J Phys Chem B 2005;109(24):11925–32.

[29] Hong CY, You YZ, Pan CY. Chem Mater 2005;17(9):2247–54.

[30] Harada A, Kataoka K. Macromolecules 1995;28(15):5294–9.

[31] Daly HW, Poche D. Tetrahedron Lett 1988;29(46):5859–62.

[32] Sunder A, Hanselmann R, Frey H, Mülhaupt R. Macromolecules 1999;32(13):4240–6.

[33] Holter D, Burgath A, Frey H. Acta Polym 1997;48(1–2):30–5.

[34] Holter D, Frey H. Acta Polym 1997;48(8):298–309.

[35] Gao C, Yan DY, Chen W. Macromol Rapid Commun 2002;23(8):465–9.

[36] Kong H, Li W, Gao C, Yan DY. J Am Chem Soc 2004;126(2):412–3.

[37] Kong H, Li W, Gao C, Yan DY. J Mater Chem 2004;14(9):1401–5.

[38] Chiu PW, Duesberg GS, Dettlaff-Weglikowska U, Roth S. Appl Phys Lett 2002;80(20):3811–3.

[39] Sano M, Kamino A, Okamura J, Shinkai S. Science 2001;293(5533):1299–301.

[40] Kong H, Li W, Gao C, Yan DY, Jin Y, Walton DRM, et al. Macromolecules 2004;37(18):6683–6.

[41] Xu GY, Wu WT, Wang YS, Pang WM, Zhu QR, Wang PH, et al. Polymer 2006;47(16):5909–18.